# Efficient Expression by an Alphavirus Replicon of a Functional Ribozyme Targeted to Human Immunodeficiency Virus Type 1

STEPHEN M. SMITH, FRANK MALDARELLI, AND KUAN-TEH JEANG*

*Laboratory of Molecular Microbiology, National Institute of Allergy and Infectious Diseases,
Bethesda, Maryland 20892-0460*

Intracellular applications of ribozymes have been limited partly by the availability of suitable high-expression systems. For RNA effectors, consideration of an RNA virus vector system for delivery and expression is reasonable. We show that alphavirus replicons can be highly efficient nonintegrating ribozyme-expressing vectors. Using a hammerhead ribozyme targeted to a highly conserved sequence in the U5 region of the human immunodeficiency virus type 1 (HIV-1) long terminal repeat, we demonstrate that a full-length 8.3-kb Semliki Forest virus ribozyme (SFVRz) chimeric RNA maintains catalytic activity. SFVRz is packaged into viral particles, and these particles transduce mammalian cells efficiently. SFVRz-transduced BHK cells were found to produce large amounts of genomic and subgenomic forms of ribozyme-containing RNAs that are functional in cleaving a U5-tagged mRNA. The RNase protection assay shows that HIV-1 U5-chloramphenicol acetyltransferase mRNA expressed intracellularly from an RNA polymerase II promoter is quantitatively eliminated in SFVRz-transduced BHK cells.

Effective use of antisense and ribozyme molecules as therapeutic and/or investigational molecules requires the intracellular attainment of a high effector-to-target stoichiometry (25). Effector expression with various "strong" promoters has resulted in limited successes (reviewed in references 3, 7, 10, 12, 13, 20, 23, and 27). Viral vectors are commonly used vehicles for introducing genetic material. One popular approach utilizes amphotropic retrovirus vectors (11). Typically, upon cellular entry, the vector migrates to the nucleus, integrates into host chromosome(s), and then either stably or conditionally expresses the effector from an internal promoter (4, 6, 18, 19, 27). While this approach has many useful features, there are circumstances in which high effector expression is desired, but vector entry or integration into host cell nuclei might be unwanted. In exploring this issue, we considered a high-expression cytoplasmic viral replicon for the synthesis of a ribozyme targeted to human immunodeficiency virus type 1 (HIV-1).

Alphaviruses are positive-strand viruses that include Sindbis (SIN) virus, Semliki Forest virus (SFV), and the human pathogens Eastern and Western equine encephalitis viruses (reviewed in reference 24). After alphaviruses enter a cell, the genomic RNA is translated to produce nonstructural (NS) proteins. The NS proteins function to produce negative-sense genome molecules from which large amounts of new genomic and subgenomic RNAs are transcribed. The subgenomic RNA, which may reach 100,000 copies per cell, codes for viral structural proteins whose assembly results in the production of progeny virions. The entire life cycle of alphaviruses takes place in the cytoplasm.

Over the past few years, recombinant alphavirus vectors have been elegantly developed for overexpression of heterologous gene products (2, 14, 21, 26). Various versions exist. Popular ones are based on SFV and SIN viruses. For these systems, nondefective and defective alphavirus replicons have been engineered, and appropriate packaging cell lines have been constructed. The efficiency of alphavirus expression is impressive, with up to 25% of total protein in infected cells being produced from the introduced vector (14). The wide host range of alphaviruses is one additional attraction of this approach (14, 22).

While users of alphavirus vectors have focused largely on their utility for protein overexpression, we reasoned that the same vectors could be valuable tools for expressing and delivering RNA effectors into cells. We thus investigated an SFV-based approach to produce a hammerhead ribozyme (SFVRz) that cleaves specifically a sequence in the U5 region of HIV-1 (6). This U5 sequence is conserved in all unspliced and spliced HIV-1 RNAs. We describe here an SFVRz replicon that efficiently eliminates intracellularly expressed HIV-1 U5 transcripts. Our results point to alphavirus vectors as nonintegrating alternatives for highly efficient expression of RNA-based effectors.

## MATERIALS AND METHODS

**Cells and cell lines.** Baby hamster kidney cells (BHK-21) (C13; ATCC, CCL 10) were maintained in Glasgow minimum essential medium (GIBCO BRL) with 10% tryptose phosphate broth–5% fetal calf serum (FCS)–10 mM HEPES (pH 7.3)–2 mM glutamine–100 U of penicillin per ml–100 μg of streptomycin per ml. A long terminal repeat (LTR) chloramphenicol acetyltransferase (CAT) cell line was created after transfection with Lipofectamine (GIBCO) of BHK-21 cells with pLTRCAT, a plasmid which has a CAT gene driven by the LTR from pNL4-3. Positive cells were selected by hygromycin selection at 300 μg/ml (Calbiochem). Clones were analyzed and found to produce CAT mRNA and protein. One clone, BHK LTR-CAT, was chosen and used for all subsequent experiments. Similarly, HeLa LTR-CAT cell clones were produced and maintained at 150 μg of hygromycin per ml (8). HeLa cells were maintained in Dulbecco's minimum essential medium (GIBCO) with 10% FCS–2 mM glutamine–100 U of penicillin per ml–100 μg of streptomycin per ml.

**Vectors.** pSFV1, pSFVlac, and pSFV-Helper 2 were obtained from GIBCO BRL. pSFVRz was constructed by placing a pair of complementary oligonucleotides (53 bp) encoding the U5 ribozyme (6) into the *Bam*HI site of pSFV. pSFVRzCD8 and pSFVCD8 were obtained by placing a PCR-generated CD8 cDNA (15) into the *Xma*I sites of pSFVRz and pSFV1, respectively. Genomic RNAs (from pSFV1, pSFVRz, pSFV3-lacZ, pSFVRzCD8, or pSFVCD8) and helper RNA (from pSFV-Helper 2) were transcribed in vitro with Sp6 RNA polymerase (GIBCO) according to the manufacturer's protocol.

**Nucleic acid analyses.** For Southern blotting, plasmid digests were separated by electrophoresis through a 1.0% agarose (FMC) gel, which was stained with ethidium bromide. DNA was transferred to nylon membrane (Schleicher & Schuell) and cross-linked by UV light. After prehybridization in 40% form-

* Corresponding author. Mailing address: Building 4, Room 306, 9000 Rockville Pike, Bethesda, MD 20892-0460. Phone: (301) 496-6680. Fax: (301) 480-3686. E-mail: kjeang@atlas.niaid.nih.gov.

amide–6× SSC (1× SSC is 0.15 M NaCl plus 0.015 M sodium citrate)–5× Denhardt's reagent–0.5% sodium dodecyl sulfate, the membrane was hybridized overnight at 42°C with a 5′-³²P-labeled DNA oligonucleotide complementary to the U5 ribozyme sequence. After being washed in 2× SSC–0.5% sodium dodecyl sulfate, the filter was visualized by autoradiography. For RNase protection assays (RPAs) after transfections or infections, cells were treated with RNAzol B (TEL-TEST, Inc.) according to the manufacturer's protocol. Total RNA was isolated. RNAs were precipitated in ethanol and pelleted. For each assay, the RNA was redissolved in water. Equivalent percentages of the total RNA were used for parallel samples. Probes were made by in vitro transcription with T7 RNA polymerase and labeled with [³²P]UTP. Approximately 5 × 10⁵ cpm of each probe was added per reaction. RPAs were performed according to the manufacturer's protocol (Ambion). In brief, cellular RNA and the RNA probe were allowed to hybridize overnight at 45°C. The mixture was then digested with RNase A (2.5 U/ml) and T₁ (100 U/ml) at 37°C for 30 min. Samples were precipitated and solubilized in gel loading buffer. RPA products were separated in a 7 M urea–6% polyacrylamide gel. The gel was dried and was visualized by autoradiography and/or phosphorimaging. Results were quantitated with a Fuji phosphorimager.

**Transfections and infections.** Following in vitro synthesis of capped genome-length RNAs, cells were electroporated with the Bio-Rad Gene Pulser at 1.25 kV, 25 μF, and infinite resistance. Cells were analyzed at the time denoted following transfection for protein and RNA. Recombinant viruses were generated by electroporating genomic RNA with helper RNA into BHK-21 cells. After 16 h, the supernatant was clarified by centrifugation, aliquoted, and frozen at −70°C. Infection of cells was performed as follows. Virions were activated by treatment with chymotrypsin (Boehringer Mannheim). Aprotinin (Sigma) was then added to terminate the protease activity. Stocks were diluted and added to the cells in the absence of serum for 1 h at 37°C. Medium was then added to the cells, which were harvested at the indicated times. The titers of viral stocks were determined, and for each experiment, 10 times the titer which achieved the highest rate of infection was used. In other words, the final titer used was 10 times more concentrated than the titer needed to infect 100% of the cells. The number of cells infected per experiment varied between 1.5 × 10⁵ and 2 × 10⁶. The cells were analyzed at the time indicated for each experiment.

**Probes.** All probes were transcribed in vitro with T7 RNA polymerase. The human actin probe (Ambion) is 188 nucleotides long and shows 125 protected nucleotides with complementary actin mRNA. The mouse actin probe (Ambion) is 300 nucleotides long and is 250 nucleotides long after protection with complementary RNA. The probe for the HIV-1 LTR was generated by cloning a fragment from pLTR-CAT in the antisense orientation to the T7 promoter in pGEM 7Z (Promega). After digestion with ClaI and transcription with T7 polymerase, the probe is 256 nucleotides long, and it is 191 nucleotides long after protection with LTR RNA. After cleavage with the U5 ribozyme, the expected sizes of the protected fragments are 111 and 80 nucleotides, respectively, for P1 and P2. A probe that overlaps the subgenomic promoter was also created from pSFVRz by PCR. This SFVRz probe is 273 bases long and yields either 195 or 177 bases when protected by genomic or subgenomic RNAs, respectively.

**Cytometry.** Cells were stained after transfection or infection with anti-CD8 (Leu-2a) phycoerythrin antibody from Becton Dickinson. Sixteen hours after transfection or infection, cells were detached from the plates and washed in phosphate-buffered saline (PBS) followed by 3% bovine serum albumin–PBS. After pelleting, the cells were resuspended in 30 μl of CD8 phycoerythrin and incubated on ice for 45 min. The cells were washed twice with PBS and analyzed by fluorescence-activated cell sorting (FACS) to determine the percentage of CD8⁺ cells.

**In situ hybridization.** Cells on glass coverslips were washed three times with PBS, fixed at room temperature for 10 min in 4% paraformaldehyde–PBS buffered to pH 7.4, washed three times in PBS, and then stored in 70% ethanol at 4°C. A biotinylated DNA probe was nick translated from pSFVRz with the Bionick kit (Life Sciences/BRL), and in situ hybridization was performed as previously described (1) with Texas red-streptavidin to detect the hybridized probe. Cells were visualized with a Zeiss LSM4 laser scanning confocal microscope (Carl Zeiss, Thornwood, N.Y.) with a 568-nm incident beam from an Ar-Kr laser to excite and a 590-nm long-pass filter to detect the fluorescence emitted by Texas red. A light microscopic image was obtained with Nomarski optics with the 568-nm incident beam. Light and fluorescent images were captured and pseudocolored (Texas red, red; light microscopy, blue).

## RESULTS

**Construction of an alphavirus ribozyme vector.** Alphavirus vectors have been used frequently for expression of foreign proteins (2, 14, 21, 26). As alluded to above, viruses with RNA genomes represent perhaps the most suitable vehicles for overexpression of RNA effectors (e.g., ribozymes). We have previously characterized a small ribozyme that cleaves a highly conserved sequence in the U5 region of the HIV-1 LTR (6, 16). Because we encountered limitations with other expression

strategies, it was of interest for us to explore alphavirus to deliver ribozymes into cells.

We positioned a small 53-nucleotide U5 ribozyme into an 8.3-kb alphavirus genome by ligating a synthetic oligonucleotide into the BamHI site of an SFV plasmid (pSFV1) to generate pSFVRz (Fig. 1A). To verify the correct insertion and configuration of the ribozyme, we performed Southern blot analysis of restricted pSFV1 and pSFVRz, and we also sequenced pSFVRz to document that the junctional and the ribozyme sequences are correct (data not shown). Both analyses showed that the ribozyme was placed correctly.

A second ribozyme-expressing SFV vector was generated by positioning a human CD8 cDNA (pSFVRzCD8) immediately 3′ to the U5 ribozyme sequence in pSFVRz (Fig. 1B). As controls for this vector, pSFV1 plasmids, without the U5 ribozyme, that express either CD8 (pSFVCD8) or the bacterial lacZ gene (pSFVlac) were also created (Fig. 1B). A feature of these vectors (see below) is that their expression in cells can be biochemically assessed by staining for either cell surface CD8 or intracellular lacZ. The former marker can be verified by FACS, while the latter can be visualized by staining with X-Gal (5-bromo-4-chloro-3-indolyl-β-D-galactopyranoside).

**An SFVRz chimeric genome is catalytically active.** Secondary structures of flanking RNAs could theoretically affect the function of an internally placed ribozyme. In our vectors, the 53-nucleotide U5 ribozyme was inserted into SFV such that there are 7.4 kb of 5′-flanking viral sequences and 0.9 kb of 3′-flanking viral sequences. Previously, it was shown that the 53-nucleotide U5 ribozyme (6) cleaves HIV-1 RNA efficiently. As a prelude to further experiments, we asked whether an 8.3-kb genome-length SFVRz chimera would retain catalytic function.

To address this question, we created a BHK cell line that constitutively expresses an integrated HIV-1 LTR-CAT plasmid. CAT mRNAs synthesized in this cell line have an HIV-1 U5 leader sequence which contains the +113 U5 ribozyme cleavage site. We developed an RPA probe such that should this CAT mRNA be cleaved by the U5 ribozyme, two product fragments (P1 and P2) with sizes of 111 and 80 nucleotides, respectively, would be generated (Fig. 2A). We then transcribed in vitro, using SP6 RNA polymerase, genome-length SFVRzCD8 RNA (8,314 nucleotides) and, using T7 RNA polymerase, a small U5 ribozyme (60 nucleotides [6]). Total cellular RNA isolated from the BHK LTR-CAT cell was then mixed with buffer (Fig. 2B, lane 1), SFVRzCD8 transcript (Fig. 2B, lane 2), or the small U5 ribozyme (Fig. 2B, lane 3). The reaction mixtures were ethanol precipitated and analyzed by RPA (Fig. 2A) followed by denaturing gel electrophoresis. Uncleaved CAT mRNA is indicated by an RPA-protected fragment with a size of 191 nucleotides (S; Fig. 2B, lane 1). In reaction mixtures containing either SFVRzCD8 (Fig. 2B; lane 2) or the small U5 ribozyme (Fig. 2B; lane 3), we observed that the 191-nucleotide species was fragmented into the two predicted products, P1 (111 nucleotides) and P2 (80 nucleotides). These results confirm that U5-CAT transcripts in a complex mixture of BHK cellular RNA can be efficiently cleaved by a ribozyme and that a genome-length SFVRzCD8 chimera maintains catalytic efficiency comparable to that of a small U5 ribozyme not flanked by SFV sequences.

**Intracellular production of SFVRzCD8.** One reason for developing an SFVRzCD8 molecule is to achieve high levels of intracellular catalytic RNA. To verify that the alphavirus vector can provide this feature, we monitored for time-dependent expression of ribozyme after transduction of BHK cells with an SFVRzCD8 genome. Replication-defective SFVRzCD8 viral particles were generated by cotransfection of SFVRzCD8 and
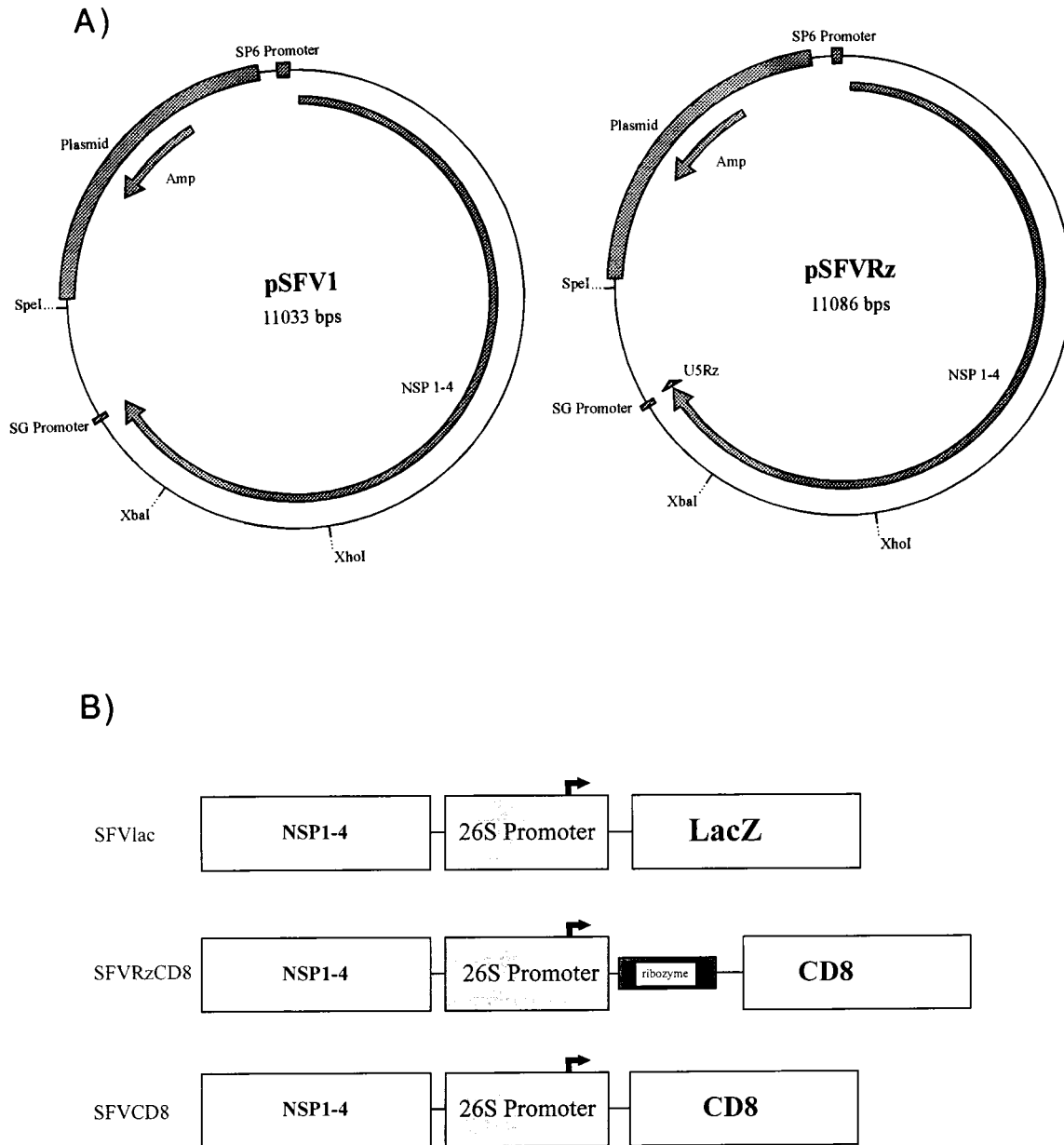
FIG. 1. Construction of vectors. (A) Schematic representations of pSFV1 (left) and pSFVRz (right). (B) Schematic linear representations of pSFVlac, pSFVRzCD8, and pSFVCD8. The 26S promoter for the transcription of subgenomic alphavirus RNAs is indicated. NSP 1–4, NS proteins 1 to 4.

SFV-Helper 2 RNAs into BHK cells. Supernatant particles (approximately $10^6$ infectious units) were then used to infect $10^5$ BHK cells. Under these conditions, we routinely achieved infection of >99% of the cells, as assessed by immunofluorescence (data not shown).

Transduced BHK cellular RNAs were sequentially harvested after exposure to virus and monitored for ribozyme production. In these experiments, because the probe spans the 26S SFV subgenomic promoter (14), genomic and subgenomic viral RNAs that contain ribozyme can be distinguished. After RNase digestion, the probe fragment protected by genomic U5 ribozyme RNA is 18 nucleotides longer than that protected by its subgenomic counterpart. In Fig. 3A, we show the profiles of intracellular ribozyme production 4 (lane 4), 8 (lane 5), and 24 (lane 6) h after virus transduction. We found that synthesis of

SFVRzCD8 RNA occurred rapidly; a strong signal was detected by 4 h after infection (Fig. 3A, lane 4). We noted that whereas the synthesis of ribozyme-containing SFVRzCD8 RNA in BHK cells was relatively constant from 4 to 24 h after infection, the ratio of genomic to subgenomic species did vary over time. In other experiments, with ethidium bromide staining and radioactive labeling of RNAs from infected cells, we estimated that SFV-specific RNAs produced from our vectors accounted for more than 1% of total RNAs (unpublished observations).

Although in vitro-transcribed SFVRzCD8 RNA is catalytically active (Fig. 2), it was important to verify that SFVRzCD8 RNA synthesized after virus transduction in the setting of a complex mixture of BHK cellular RNAs is similarly active. One way to answer this question is to assay directly for ribozyme
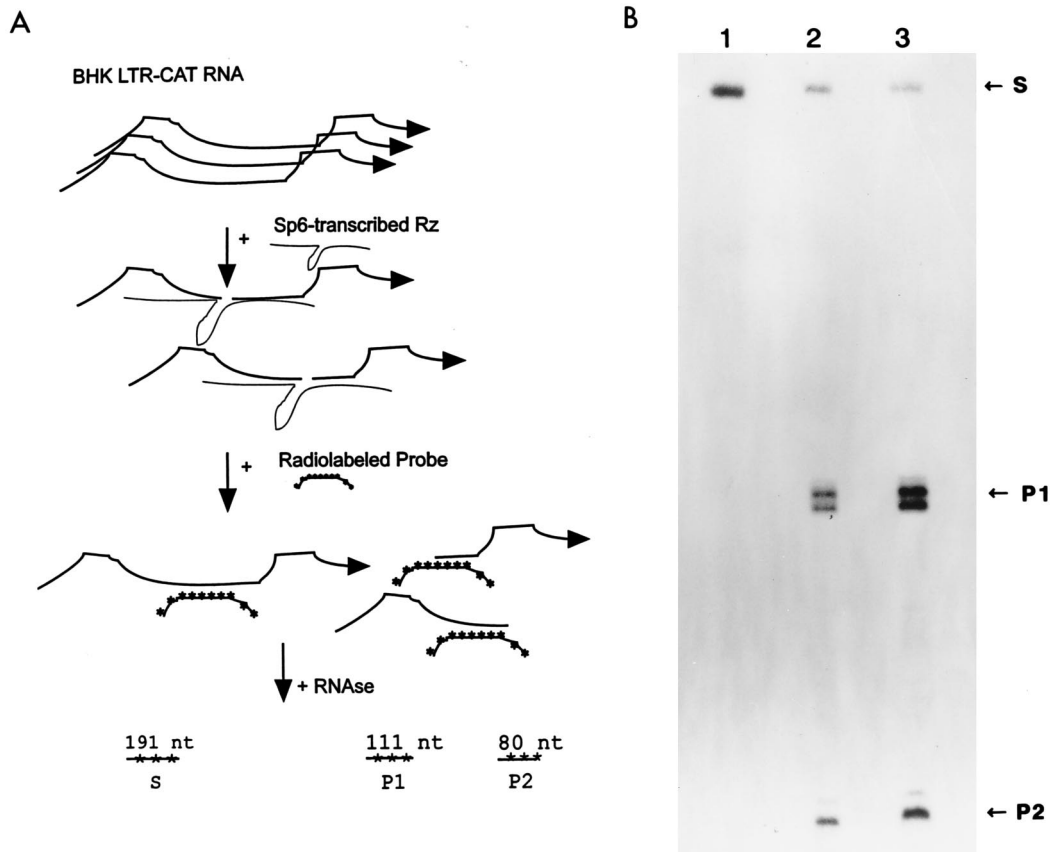
FIG. 2. An 8.3-kb SFVRz chimeric RNA maintains the same catalytic activity as a small U5 ribozyme. (A) Schematic illustration of an RPA that discriminates between probe-protected uncleaved CAT mRNA substrate (S; 191 nucleotides [nt]) and ribozyme-generated cleavage products (P1 and P2; 111 and 80 nucleotides, respectively). (B) RPA analysis demonstrating ribozyme activity in SFVRz chimeric RNA. A 60-nucleotide control U5 ribozyme (lane 3) or an 8.3-kb SFVRz RNA (lane 2) was transcribed in vitro. BHK LTR-CAT total-cell RNA was isolated and used as a substrate. The BHK LTR-CAT total-cell RNA was mixed with buffer (lane 1), SFVRz RNA (lane 2), or the 60-nucleotide U5 ribozyme. Cleavage of the U5-CAT mRNA present in BHK LTR-CAT total-cell RNA was monitored by RPA followed by denaturing gel electrophoresis and autoradiography. Both SFVRz RNA (lane 2) and control U5 ribozyme (lane 3) produced the expected cleavage products, P1 (111 nucleotides) and P2 (80 nucleotides). Buffer alone (lane 1) produced no cleavage of substrate.

activity of intracellular SFVRzCD8 RNA. To do this, we synthesized in vitro a uniformly [$^{32}$P]UTP-labeled, 754-nucleotide substrate RNA (S; Fig. 3B) which spans a cleavage-sensitive site. In parallel, we also transcribed a small U5 ribozyme (Fig. 3B, lane 2) for use as a positive control. As test ribozymes, we isolated total cellular RNA from BHK cells transduced with either replication-defective SFVRzCD8 (Fig. 3B, lane 4) or SFVCD8 (Fig. 3B, lane 3) particles. SFVRzCD8 RNA would represent a small minority of total BHK SFVRzCD8 cellular RNA, and we reasoned that a good test would be whether we could document ribozyme activity in this mixture of cellular RNAs.

We incubated the 754-nucleotide RNA substrate (S; Fig. 3B) with buffer (Fig. 3B, lane 1), with in vitro-synthesized small U5 ribozyme (Fig. 3B, lane 2), or with total RNA from BHK cells transduced with either SFVCD8 (Fig. 3B, lane 3) or SFVRzCD8 (Fig. 3B, lane 4) virus. Each mixture was subjected to 10 cycles (37°C for 2 min and then 65°C for 2 min) of in vitro ribozyme cleavage as previously described (5). Equivalent amounts of reaction material were then resolved by denaturing gel electrophoresis, and cleavage of substrate was assessed by visualization for the generation of product RNAs (P1, 575 nucleotides; P2, 179 nucleotides [Fig. 3B]). We found that while total cellular RNA from BHK cells transduced with SFVCD8 showed no substrate-cleaving activity (Fig. 3B; lane

3), both the small control U5 ribozyme (Fig. 3B; lane 2) and total cellular RNA from BHK cells transduced with SFVRzCD8 (Fig. 3B, lane 4) cleaved the target RNA. This verifies that SFVRzCD8 RNA, despite being a small portion in a complex mixture of cellular RNAs, maintains specific U5-cleaving activity.

SFVRzs should affect target RNAs without exhibiting nonspecific cleavage and toxicity for other intracellular RNAs. To assess this, we checked for the steady-state synthesis and stability of a prototypic cellular mRNA (actin) in mock- and SFVRzCD8-infected BHK cells (Fig. 3C) 24 h after infection. Total RNAs were isolated from the former (Fig. 3C, lanes 3 and 7) and the latter (Fig. 3C, lanes 4 and 8) and were analyzed with either actin- (Fig. 3C, lanes 3 and 4) or ribozyme (Fig. 3C, lanes 7 and 8)-specific probes. Abundant ribozyme expression was documented in SFVRzCD8-infected (Fig. 3C, lane 8) but not in mock-infected (Fig. 3C, lane 7) BHK cells. However, the steady-state appearances of actin mRNA in the two types of cells were indistinguishable (Fig. 3C, compare lanes 3 and 4). Thus, at this level of resolution, the specificity of SFVRzCD8 is such that, metabolically, other cellular RNAs are not adversely perturbed.

**Efficacy of SFVRz in cells.** In principle, the SFVRz genome permits de novo transcription of ribozyme from the subgenomic 26S viral promoter. To assess whether such amounts
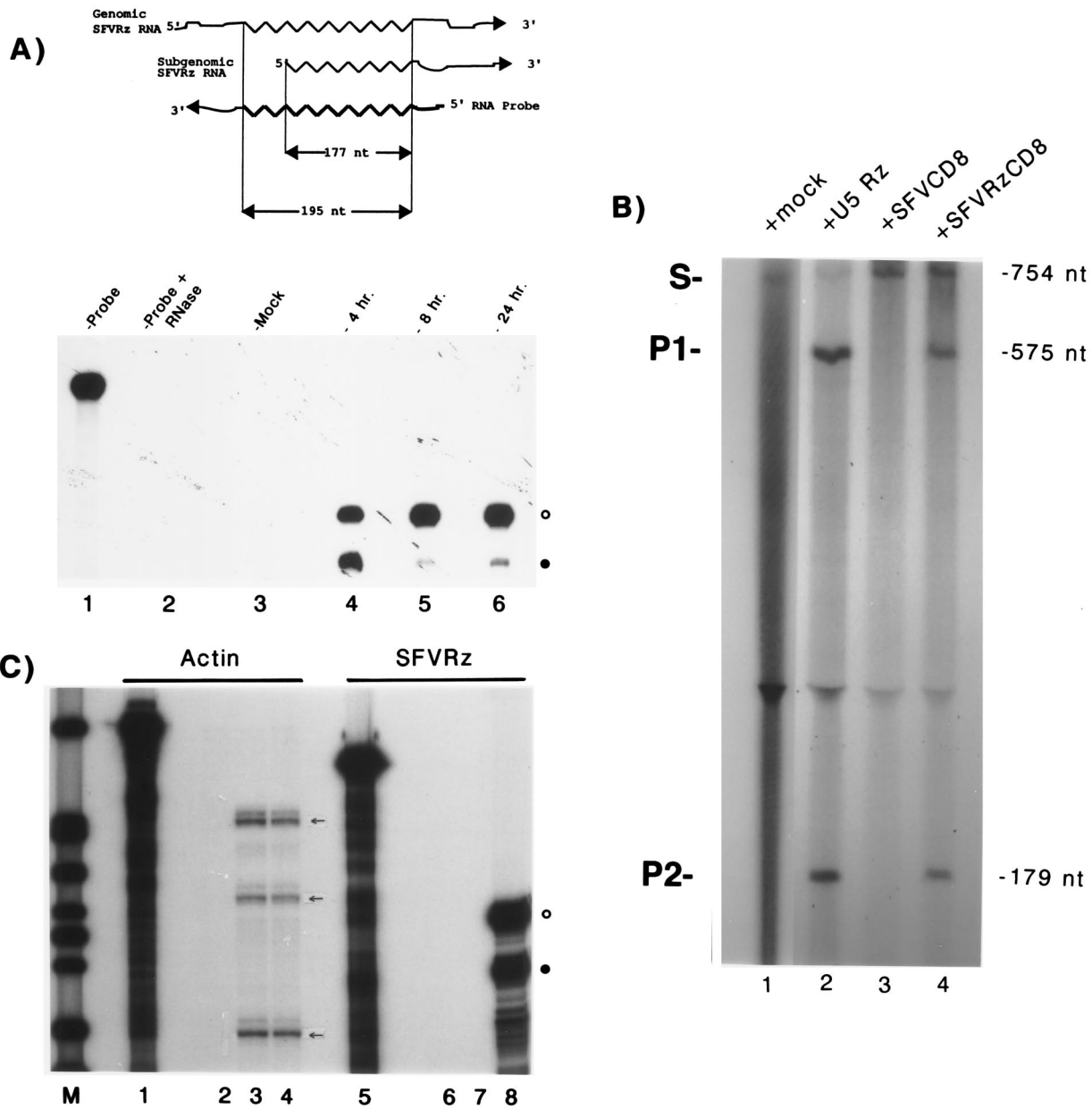
FIG. 3. Rapid synthesis of catalytically active RNA follows SFVRz transduction. (A) RPA analysis of ribozyme activity. (Top) Schematic representation of probe that discriminates between SFVRz-containing transcripts in genomic (195 nucleotides [nt]) or subgenomic (177 nucleotides) forms. (Bottom) Time course of SFVRz production following transduction. BHK cells were transduced with SFVRz particles. Total RNA was isolated 4, 8, and 24 h later and analyzed by RPA. Lanes 1 and 2 show the probe alone without and with RNase treatment, respectively. Lane 3 shows the results of RPA analysis of mock-transduced BHK total RNA. BHK SFVRzCD8 cells show strong ribozyme signals at 4 (lane 4), 8 (lane 5), and 24 (lane 6) h after transduction. The intensities of the ribozyme signals are roughly equivalent, but the ratio of genomic (open circle) to subgenomic (solid circle) forms varied over time. (B) Characterization of catalytic activity in SFVRzCD8 RNA synthesized in BHK cells. HIV LTR RNA (substrate [S]) was transcribed and labeled with [$^{32}$P]UTP in vitro. S (754 nucleotides) was mixed with buffer (lane 1), a small control U5 ribozyme (lane 2), or total-BHK-cell RNA isolated 24 h after transduction with either SFVCD8 (lane 3) or SFVRzCD8 (lane 4) particles. Each reaction mixture was incubated for 10 cycles of ribozyme cleavage as previously described (5) and analyzed by denaturing gel electrophoresis. Both control U5 ribozyme (lane 2) and cell RNA from BHK SFVRzCD8 transduction (lane 4) cleaved S to the expected products, P1 (575 nucleotides) and P2 (179 nucleotides). Transduction with SFVCD8 produced no ribozyme activity in BHK cell RNA (lane 3). A total of 250 ng of control U5 ribozyme was used in lane 2. Judging by the relative cleavage intensities, we estimate that the total cellular RNA from SFVRzCD8 cells (lane 4) contains no more than 25 ng eq of U5 ribozyme activity. (C) Stability of actin mRNA in BHK cells 24 h after transduction with SFVRzCD8 particles. Lane 1 contains actin probe alone, lane 2 contains the actin probe digested with RNase, lane 5 contains SFVRz probe alone (A), and lane 6 contains SFVRz probe after digestion with RNase. Results from RPAs of total-cell RNA from mock-infected cells with actin (lane 3)- or ribozyme (lane 7)-specific probe are compared with those from analysis of total-cell RNA from SFVRzCD8-transduced cells obtained with an actin (lane 4)- or ribozyme (lane 8)-specific probe. Arrows point to protected bands that are produced when murine actin probe is used to assay hamster (BHK) cell actin mRNA. Comparison of lanes 7 and 8 verifies that abundant synthesis of SFVRz (genomic, open circle; subgenomic, solid circle) RNAs is found in SFVRzCD8-transduced BHK cells. Of note, the steady-state level of actin in lane 4 is essentially unchanged from that in lane 3. Lane M, molecular size markers ($^{32}$P-end-labeled pBR322/MspI fragments).
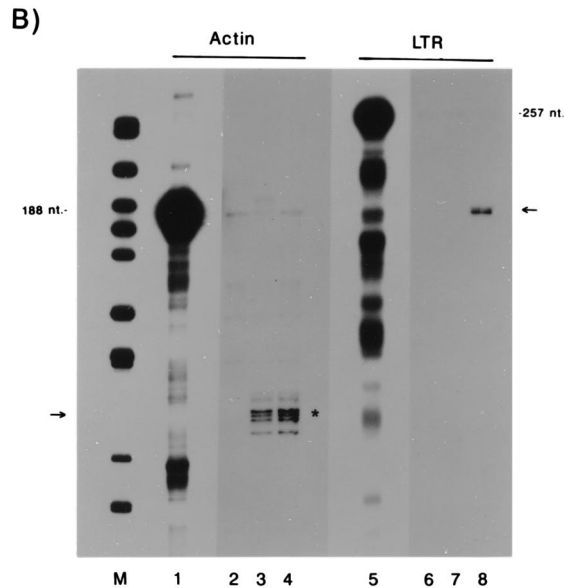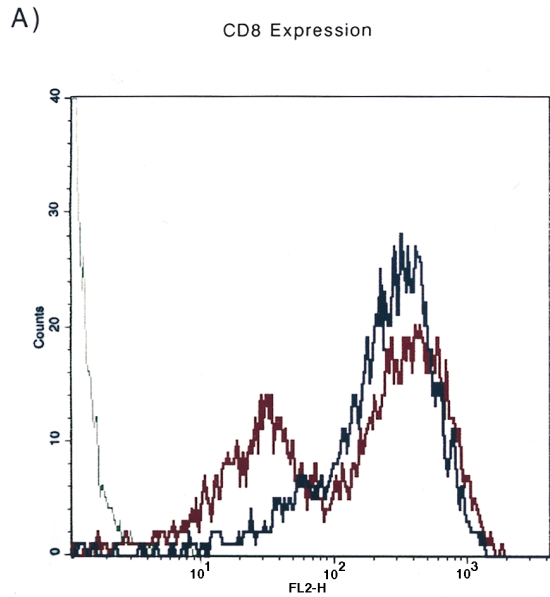
A)

CD8 Expression



FIG. 4. Intracellular efficacy of electroporated SFVRzCD8 ribozyme. (A) FACS analysis of cell surface CD8 expression. HeLa LTR-CAT cells were electroporated with SFVRzCD8 RNA, SFVCD8 RNA, or buffer. Sixteen hours later, cells were stained for surface CD8 and analyzed by FACS. The majority of SFVRzCD8 (red)- and SFVCD8 (blue)-electroporated cells, compared with the buffer (green)-electroporated cells, showed high levels of CD8 expression. A fluorescence gate value was set at FL2-H of $10^2$; cells staining with intensities above this value were collected. (B) RPA analysis of CD8-enriched HeLa LTR-CAT cells. Lanes 3 and 4 show the results from an RPA using the human actin probe of total-cell RNA from SFVRzCD8 (lane 3) or SFVCD8 (lane 4) cells. The asterisk indicates the expected protection fragments. Lane 1 contains the input actin probe; lane 2 contains the input actin probe after digestion with RNase. Lanes 7 and 8 contain the same RNA samples as lanes 3 and 4, except that here the intactness of LTR-CAT mRNA was assessed with an HIV-1 LTR-specific RNA probe (lane 5). The arrow points to the protection seen for uncleaved LTR-CAT mRNA. Lane 6 is lane 5 after digestion with RNase. (C) Activity of ribozyme in BHK LTR-CAT cells. BHK LTR-CAT cells were transfected with either SFVlac or SFVRz genomic RNA. After 16 h, the cells were harvested, protein was extracted, and the CAT assay was performed. SFVlac-transfected cells showed 8.5% acetylation, while SFVRz-transfected cells showed 3.2% acetylation. The transfection efficiency of SFV genomes was >95%, as demonstrated by X-Gal staining of a parallel culture.

B)



C)
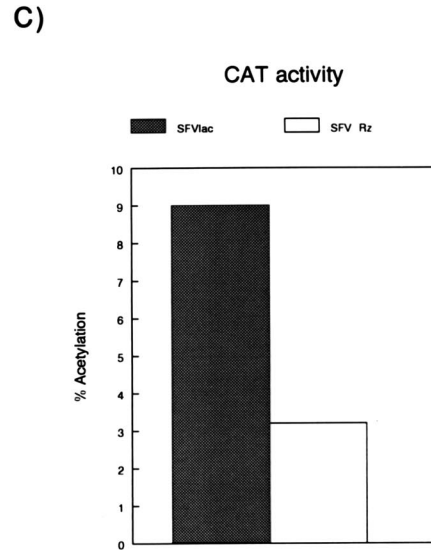


of ribozyme synthesis would be sufficiently effective against U5 RNAs expressed intracellularly from a polymerase II promoter, we electroporated either SFVRzCD8 or SFVCD8 genomes into a HeLa LTR-CAT cell line. This cell line synthesizes constitutively CAT mRNAs tagged with a U5 ribozyme cleavage site. Because both SFVRzCD8 and SFVCD8 RNAs were engineered to express CD8 (Fig. 1C), introduction of either into cells should result in cell surface expression of CD8 antigen. Sixteen hours after electroporation, cells staining for CD8 were checked by FACS. In both sets, over 95% of the electroporated cells stained positively for CD8 (Fig. 4A). While SFVCD8 cells (blue curve, Fig. 4A) showed one predominantly stained peak, the SFVRzCD8 cells (red curve, Fig. 4A) produced two populations of CD8-expressing cells, both expressing levels of CD8 considerably higher than the background staining seen in control cells (green curve, Fig. 4A). The reason(s) for the appearance of two populations in SFVR zCD8 cells is not clear (possibilities include reduction in CD8

translation from steric interference caused by the secondary structure of the U5 ribozyme or interference by a fortuitous ATG trinucleotide [5′ to the CD8 ATG] contained within the U5 ribozyme sequence), but this pattern was reproducibly seen.

The CD8 surface marker allows for efficient "sorting" of HeLa LTR-CAT cells that have received SFV genomes. We sorted cells by using a fluorescence gate set at a signal intensity $10^2$-fold higher than that from control nonelectroporated cells. After being enriched for CD8 cells, total cellular RNAs were harvested, and amounts of U5-containing CAT RNA were quantified by RPA. We compared RNAs from HeLa LTR-CAT cells that received either SFVRzCD8 (Fig. 4B, lanes 3 and 7) or SFVCD8 (Fig. 4B, lanes 4 and 8), probing for either actin (Fig. 4B, lanes 2 to 4) or CAT (Fig. 4B, lanes 6 to 8) mRNA. While the levels of actin mRNA stayed approximately constant between SFVRzCD8 (Fig. 4B, lane 3) and SFVCD8 (Fig. 4B, lane 4) cells, the ratio of CAT to actin RNA was
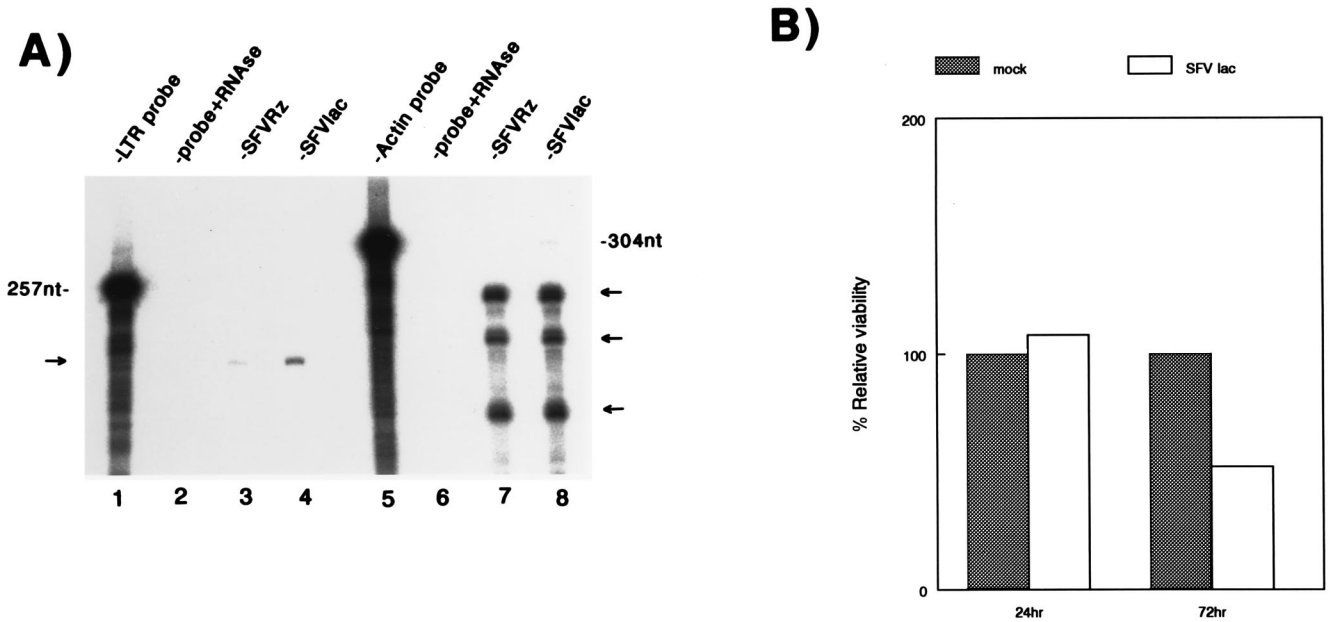
FIG. 5. Intracellular efficacy of virally transduced SFVRz. (A) BHK LTR-CAT cells were transduced with SFVRz or SFVlac viral particles. Total RNAs were harvested 16 h later and analyzed with LTR (lanes 3 and 4)- or actin (lanes 7 and 8)-specific probes. An RPA with the LTR-specific probe shows significantly reduced amounts of LTR-CAT mRNA in SFVRz (lane 3)- versus SFVlac (lane 4)-transduced cells. Control RPA with a murine actin probe shows equivalent actin mRNA signals in the SFVRz (lane 7) and SFVlac (lane 8) samples. Lanes 1 and 5 contain input LTR and actin probes, respectively. Lanes 2 and 6 contain the same probes digested with RNase. (B) Time course of cell viability. BHK cells were mock transfected or transfected with SFVlac. Cells were scraped 24 and 72 h after transfection and counted for trypan blue exclusion. For the same number of total cells, the percentages of viable cells in the SFVlac sample were 108% compared to that of the control at 24 h and 52% compared to that of the control at 72 h.

decreased by 97% in SFVRzCD8 cells compared to that in SFVCD8 (Fig. 4B; compare lane 6 to lane 7) cells. This level of intracellular efficacy is considerably better than that achieved previously with the same ribozyme (6), thus confirming an increased expression capacity with SFV vectors. The efficiency of the ribozyme was also assessed at the level of CAT protein. In this case, we transfected a BHK LTR-CAT cell line at >95% efficiency with either the SFVlac or SFVRz (Fig. 4C) genome. CAT activities, determined 16 h after transfection, showed a 62% reduction in the presence of the SFVRz ribozyme. The apparently reduced efficiency of the ribozyme in the protein assay is likely a reflection of the stability of presynthesized CAT protein.

For practical applications, viral infection, rather than RNA transfection, is more likely to be used. Hence, we assessed targeting of intracellular RNA when SFVRz is transduced into cells with viral particles. We generated replication-defective SFVRz and SFVlac (Fig. 1B) viruses by using SFV-Helper 2 RNA (GIBCO BRL). After being optimized for viral titer (usually $10^6$ particles was sufficient to achieve close to 100% infection of $10^5$ BHK cells), we quantatively transduced BHK LTR-CAT cells with either SFVRz or SFVlac. Sixteen hours later, total RNAs were extracted and analyzed by RPA with an LTR (Fig. 5A, lanes 2 to 4)- or actin (Fig. 5A, lanes 6 to 8)-specific probe. (Multiply protected bands are produced (see Fig. 5A, lanes 7 and 8) when a murine-specific actin probe is used to assay hamster cell RNAs.) A comparison between the RNA samples revealed that whereas the intensities of actin were essentially invariant (Fig. 5A, compare lane 7 to lane 8), the amount of LTR-specific RNA in SFVRz-transduced cells (Fig. 5A, lane 3) was reduced by greater than 75% compared to that seen in the SFVlac sample (Fig. 5A, lane 4). This level of efficacy mirrors that achieved by RNA transfection (Fig. 4) followed by enrichment. However, the efficiency of delivery via

infection obviates the need to enrich for cells based on a selectable and visualizable (e.g., CD8) marker. Thus, high-efficiency transduction of cells and high levels of expression upon entry into cells make SFV an attractive vector system for ribozymes.

As shown in Fig. 5B, we reexamined the issue of SFV toxicity for cells. Here BHK cells were transfected at >95% efficiency with the SFVlac genome (as visualized by X-Gal staining of a parallel cell culture). Cells were then harvested 24 and 72 h after transfection; viability was assessed by trypan blue exclusion. The results showed that 24 h after introduction of the viral genome into cells (a time point at which most of our ribozyme efficacy assays were performed), no cellular toxicity was observed.

**Subcellular localization of SFVRz activity.** As an alphavirus, SFV transcripts are expected to be cytoplasmic. Experimentally, if SFVRz chimeras were to conform strictly to this expectation, then this vector system could be used selectively in settings in which one wishes to target only the cytoplasmic but not the nuclear version of an RNA. To check intracellular ribozyme localization, we performed in situ RNA hybridization followed by confocal imaging (Fig. 6). BHK cells were mock electroporated or electroporated with SFVRz RNA. Forty-eight hours later (at which point, input RNAs are degraded [data not shown]), cells were fixed with paraformaldehyde and hybridized in situ with a fluorescent single-stranded DNA probe complementary to the ribozyme. Representative images are shown in Fig. 6. We found that SFVRzs stained in a nuclearly excluded pattern consistent with exclusive localization in the cytoplasm. This observation is consistent with the expected expression profile for alphaviruses; it suggests that in settings in which target RNAs are found in both nuclear and cytoplasmic compartments, SFVRzs can be expected to degrade selectively the latter moieties.
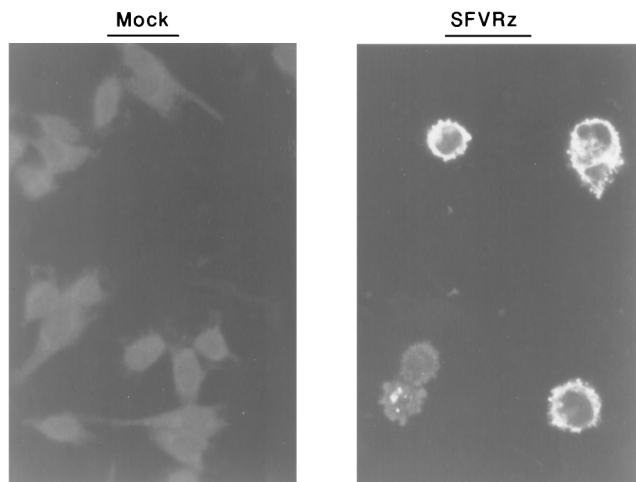
FIG. 6. Localization of SFVRz RNA in the cytoplasm. Confocal imaging was performed with mock- and SFVRz-electroporated BHK cells. Forty-eight hours after electroporation, cells were hybridized with a single-stranded SFVRz-complementary fluorescent DNA probe and visualized in situ. (A) Mock-electroporated cells. (B) SFVRz-electroporated cells. The staining pattern is consistent with ribozyme RNA being localized exclusively in the cytoplasm.

## DISCUSSION

We have tested the utility of an SFV replicon for functional intracellular expression of a hammerhead ribozyme. We concluded that (i) alphavirus vectors are highly efficient nonintegrating vehicles for ribozyme expression and (ii) expression of an SFVRz RNA produces catalytically specific intracellular activity with minimal nonspecific effects on nontargeted RNAs. While our functional results are consistent with ribozyme activity, we do not exclude some contribution from antisense and aptamer effects.

There are three reasons to consider alphavirus vectors for ribozyme expression. First, the entire life cycle of alphavirus is RNA based. Hence, in theory, both genomic and subgenomic alphavirus transcripts could be engineered to have catalytic activity. In practice, we found that a small ribozyme inserted into a larger SFV genome retains catalytic activity in genomic and subgenomic SFVRz chimeric transcripts. Thus, ribozyme activity could be generated for all stages of the alphavirus life cycle. A second reason for consideration is the broad host range of alphaviruses. Alphaviruses replicate in many tissues, including neurons. Different alphaviruses show slightly different tropism for some tissues compared to others (reviewed in reference 9). Hence, collectively, SFV- and SIN-based replicons potentially afford a biologically versatile array of tools for cellular targeting. The third and probably most persuasive reason to consider alphavirus vectors is their tremendously high levels of expression. More than 100,000 copies of alphavirus transcripts can be generated per infected cell (24). This, more than any other factor, likely accounts for the observed intracellular efficacy of our SFV U5 ribozyme. One practical concern is that expression of a foreign gene product or products to such a degree cannot be benign for the host cells. Indeed, alphavirus-mediated host cell shutoff has been well described (24). Interestingly, in our assays, we did not see much generalized cytotoxicity (as measured by actin mRNA metabolism and trypan blue exclusion) until 72 h after the introduction of our SFVRz replicons. It is possible that in certain settings, cytotoxicity is largely a consequence of host ribosomal cooptation by overexpressed viral mRNAs. Hence, expression of

catalytic RNAs (that are not translated) would be less toxic than that of protein-coding mRNAs for the host cell.

In comparing the SFV approach to other methods, we point to our previous experience in expressing the same HIV-1 U5 ribozyme with a retrovirus-based system (6). Although both approaches use RNA-virus vectors, the two methods have important differences. A potentially important advantage of SFV is its cytoplasmic life cycle and the fact that it does not have a DNA intermediate. Hence, at no stage in the SFV life cycle (including the initial production of virion stock with in vitro-transcribed genomic RNA) is a DNA form encountered. In situations in which insertional mutagenesis might be a concern, neither highly efficient retrovirus integrase-mediated nor low-probability stochastic chance integration of DNA into the host chromosome needs to be a source of worry with SFV vectors. Indeed, our empirical findings demonstrate that chimeric SFV nucleic acids are tightly restricted to the cytoplasm (Fig. 6).

We show the SFV replicon to be an excellent tool for transient expression of RNA effectors. In the overall picture of gene therapy, transient vectors clearly have a role. The extent of this role is not evident, since little has been done to investigate specifically transient RNA-based vectors in gene therapy (17). In settings in which permanence in therapy is not needed, such vectors permit a time-limited delivery of a transient phenotype to a host. Possibly, under limited circumstances, a transient phenotype therapy could suffice in toto or be useful as adjunct treatment. For therapy of longer duration, for this approach, one looks to noncytopathic forms of alphavirus (reviewed in reference 9) that can be used for chronic infections.

## REFERENCES

1. Berthold, E., and F. A. Maldarelli. 1996. cis-Acting elements in human immunodeficiency virus type 1 RNAs direct viral transcripts to distinct intranuclear locations. J. Virol. 70:4667–4682.
2. Bredenbeek, P. J., and C. M. Rice. 1992. Animal RNA virus expression systems. Semin. Virol. 3:297–310.
3. Cech, T. R. 1993. The efficiency and versatility of catalytic RNA: implications for an RNA world. Gene 135:33–36.
4. Cotten, M., and M. L. Birnstiel. 1989. Ribozyme mediated destruction of RNA in vivo. EMBO J. 8:3861–3866.
5. Dropulic, B., N. H. Lin, and K. T. Jeang. 1993. A method to increase the cumulative cleavage efficiency of ribozymes: thermal cycling. Nucleic Acids Res. 21:2273–2274.
6. Dropulić, B., N. H. Lin, M. A. Martin, and K.-T. Jeang. 1992. Functional characterization of a U5 ribozyme: intracellular suppression of human immunodeficiency virus type 1 expression. J. Virol. 66:1432–1441.
7. Dropulic, B., S. M. Smith, and K. T. Jeang. 1994. Activation and inactivation of gene expression using RNA sequences. Adv. Pharmacol. 30:247–270.
8. El Kharroubi, A., and M. A. Martin. 1996. cis-Acting sequences located downstream of the human immunodeficiency virus type 1 promoter affect its chromatin structure and transcriptional activity. Mol. Cell. Biol. 16:2958–2966.
9. Frolov, I., T. A. Hoffman, B. M. Pragai, S. A. Dryga, H. V. Huang, S. Schlesinger, and C. M. Rice. 1996. Alphavirus-based expression vectors: strategies and applications. Proc. Natl. Acad. Sci. USA 93:11371–11377.
10. Homann, M., S. Tzortzakaki, K. Rittner, G. Sczakiel, and M. Tabler. 1993. Incorporation of the catalytic domain of a hammerhead ribozyme into antisense RNA enhances its inhibitory effect on the replication of human immunodeficiency virus type 1. Nucleic Acids Res. 21:2809–2814.
11. Israel, M. 1993. Molecular approaches to cancer therapy. Adv. Cancer Res. 61:57–85.
12. Kashani-Sabet, M., T. Funato, V. A. Florenes, O. Fodstad, and K. J. Scanlon. 1994. Suppression of the neoplastic phenotype in vivo by an anti-ras ribozyme. Cancer Res. 54:900–902.
13. Kashani-Sabet, M., T. Funato, T. Tone, L. Jiao, W. Wang, E. Yoshida, B. I. Kashfinn, T. Shitara, A. M. Wu, and J. G. Moreno. 1992. Reversal of the malignant phenotype by an anti-ras ribozyme. Antisense Res. Dev. 2:3–15.

14. **Liljestrom, P., and H. Garoff.** 1991. A new generation of animal cell expression vectors based on the Semliki Forest virus replicon. Bio/Technology **9:**1356–1361.
15. **Littman, D. R., Y. Thomas, P. J. Maddon, L. Chess, and R. Axel.** 1985. The isolation and sequence of the gene encoding T8: a molecule defining functional classes of T lymphocytes. Cell **40:**237–246.
16. **Lustig, B. N., N. H. Lin, S. M. Smith, R. L. Jernigan, and K. T. Jeang.** 1995. A small modified hammerhead ribozyme and its conformational characteristics determined by mutagenesis and lattice calculation. Nucleic Acids Res. **23:**3531–3538.
17. **Mebatsion, T., M. J. Schnell, J. H. Cox, S. Finke, and K. K. Conzelmann.** 1996. Highly stable expression of a foreign gene from rabies virus vectors. Proc. Natl. Acad. Sci. USA **93:**7310–7314.
18. **Paulus, W., I. Baur, F. M. Boyce, X. O. Breakefield, and S. A. Reeves.** 1996. Self-contained, tetracycline-regulated retroviral vector system for gene delivery to mammalian cells. J. Virol. **70:**62–67.
19. **Rossi, J. J., D. Elkins, N. Taylor, J. A. Zaia, S. Sullivan, and J. O. Deshler.** 1991. Exploring the use of antisense enzymatic RNA molecules (ribozymes) as therapeutic agents. Antisense Res. Dev. **1:**285–288.
20. **Sarver, N., E. M. Cantin, P. S. Chang, J. A. Zaia, P. A. Ladne, D. A.** Stephens, and J. J. Rossi. 1990. Ribozymes as potential anti-HIV-1 therapeutic agents. Science **247:**1222–1225.
21. **Schlesinger, S.** 1993. Alphaviruses—vectors for the expression of heterologous genes. Trends Biotechnol. **11:**18–22.
22. **Schlesinger, S.** 1995. RNA viruses as vectors for the expression of heterologous proteins. Mol. Biotechnol. **3:**155–165.
23. **Steinecke, P., T. Herget, and P. H. Schreier.** 1992. Expression of a chimeric ribozyme gene results in endonucleolytic cleavage of target mRNA and a concomitant reduction of gene expression in vivo. EMBO J. **11:**1525–1530.
24. **Strauss, J. H., and E. G. Strauss.** 1994. The alphaviruses: gene expression, replication, and evolution. Microbiol. Rev. **58:**491–562.
25. **Wang, S., and B. J. Dolnick.** 1993. Quantitative evaluation of intracellular sense: antisense RNA hybrid duplexes. Nucleic Acids Res. **21:**4383–4391.
26. **Xiong, C., R. Levis, P. Shen, S. Schlesinger, C. M. Rice, and H. V. Huang.** 1989. Sindbis virus: an efficient, broad host range vector for gene expression in animal cells. Science **243:**1188–1191.
27. **Yu, M., J. Ojwang, O. Yamada, A. Hampel, J. Rapapport, D. Looney, and F. Wong-Staal.** 1993. A hairpin ribozyme inhibits expression of diverse strains of human immunodeficiency virus type 1. Proc. Natl. Acad. Sci. USA **90:**6340–6344.